

## Multipair excitations and sum rules in interacting-electron systems

F. Green and D. Neilson

*School of Physics, The University of New South Wales, Kensington, Sydney 2033, Australia*

D. Pines

*Department of Physics, University of Illinois at Champaign-Urbana, 1110 West Green Street, Urbana, Illinois 61801*

J. Szymański

*Telecom Australia Research Laboratories, 770 Blackburn Road, Clayton 3168, Australia\**  
*and School of Physics, The University of New South Wales, Kensington, Sydney 2033, Australia*

(Received 17 June 1986)

Multipair excitations in the interacting-electron gas at metallic densities are quantitatively investigated at large momentum transfers with use of the microscopic Green-Neilson-Szymański (GNS) theory. The effect of single-pair and multipair excitations on the dynamic response function  $\chi(q, \omega)$  are contrasted, and the relative strengths of these excitations are compared. It is shown that the multiple-peak structures in the dynamic structure factor  $S(q, \omega)$  as calculated in the GNS theory are associated with pure multipair effects. The essential role multipair effects play in determining the high-energy-transfer tail of  $S(q, \omega)$  is stressed, and the way this affects the frequency moment sum rules is examined. Other properties of these sum rules, when they are generated within approximate but conserving theories, are discussed.

### I. INTRODUCTION

Multipair fluctuations of an interacting-fermion system consist of the simultaneous excitation of two or more quasiparticles out of the ground state. Some twenty five years ago Miller, Nozières, and Pines<sup>1</sup> emphasized the importance of multipair excitations in determining the dynamic structure factor  $S(q, \omega)$  of <sup>4</sup>He at very low temperatures. If one neglects the possibility of two or more quasiparticles being excited out of the condensate, one can then use the  $f$ -sum rule to recover the well-known Feynman result<sup>2</sup> for the single-phonon spectrum  $\omega_q = q^2/2mS(q)$ , where  $S(q)$  is the static structure factor. By adopting a phenomenological treatment of the multipair excitations it is possible to recover the experimental dispersion curve for  $\omega_q$ . Recently Manousakis, Pines, and Usmani<sup>3</sup> used the constraints imposed by the  $f$ -sum rule and the higher moment frequency sum rules to calculate the multipair contributions.

In the case of the interacting-electron gas at metallic densities, the well-known breakdown of the random-phase approximation (RPA) at metallic densities is not by itself evidence of the importance of dynamic multipair excitations for this system. The reason is the following. The primary cause of the breakdown of the RPA is that it fails to take into account the effect of electron-electron correlations on the Coulomb interaction  $V(q)$  at short distances. A static local field correction  $g(q)$  can be constructed to approximately include the effect of these correlations.<sup>4</sup> Provided  $g(q)$  is real and static, no dynamic multipair effects can be present. This is most easily demonstrated by reformulating the theory as an RPA theory with an effective interaction between electrons  $V_{\text{eff}}(q) = V(q)[1 - g(q)]$ . It is only when the local field is

permitted to develop an imaginary component, or alternatively, when it becomes a dynamic function of the energy transfer  $\omega$ , that dynamic multipair effects appear in the theory.<sup>5</sup>

Iwamoto, Krotscheck, and Pines<sup>6</sup> used the results of the Monte Carlo calculations of Ceperley and Alder<sup>7</sup> to graphically demonstrate this point. Recall the expression for the proper density-density response function

$$\chi^{\text{sc}}(q, \omega) = \frac{\chi^{(0)}(q, \omega)}{1 + V(q)g(q)\chi^{(0)}(q, \omega)}, \quad (1)$$

where  $\chi^{(0)}(q, \omega)$  is the response function for the noninteracting system, the Lindhard function. The dynamic structure factor is related to  $\chi^{\text{sc}}(q, \omega)$  through the expression

$$S(q, \omega) = -\frac{1}{\pi} \frac{\text{Im}\chi^{\text{sc}}(q, \omega)}{|1 - V(q)\chi^{\text{sc}}(q, \omega)|^2}. \quad (2)$$

Iwamoto, Krotscheck, and Pines constructed a static local field  $g(q) = G_{\text{MC}}(q)$  to reproduce the structure factor  $S_{\text{MC}}(q)$  as calculated by Ceperley and Alder for momentum transfers  $q \geq k_F/2$ . For smaller values of the momentum transfer, the numerical values from the Monte Carlo (MC) calculation have some uncertainty associated with them, but for this case there is an expression which can be used for  $g(q)$  which is known to be exact in the long-wavelength limit. Substituting the resultant static and dynamic structure factors in the third-frequency-moment sum rule, Iwamoto, Krotscheck, and Pines found significant violations throughout the metallic density range. They then pointed out that an alternative local field  $G_3(q)$  can be constructed using the same Monte Carlo data. We recall that the third-moment sum rule can be written (units are such that  $\hbar = m = 1$ )

$$\int_0^\infty S(q, \omega) \omega^3 d\omega = nq^2 \left[ \frac{q^4}{8} + q^2 \langle E_{\text{kin}} \rangle + \frac{\omega_p^2}{2} [1 - I(q)] \right], \quad (3)$$

where  $n$  is the average particle density,

$$I(q) = \frac{1}{N} \sum_{\mathbf{k}} (\hat{\mathbf{q}} \cdot \hat{\mathbf{k}})^2 [S(k) - S(|\mathbf{q} - \mathbf{k}|)],$$

and  $\langle E_{\text{kin}} \rangle$  is the expectation value of the kinetic energy in the interacting system. The sum rule can be reexpressed using Eq. (1) as

$$\int_0^\infty S(q, \omega) \omega^3 d\omega = nq^2 \left[ \frac{q^4}{8} + q^2 \langle E_{\text{kin}} \rangle_0 + \frac{\omega_p^2}{2} [1 - g(q)] \right], \quad (4)$$

where the expectation value  $\langle E_{\text{kin}} \rangle_0$  here is for the noninteracting electron gas. A comparison of Eqs. (3) and (4) reveals that the third-frequency-moment sum rule will be satisfied provided

$$g(q) = G_3(q) = I(q) - \frac{2q^2}{\omega_p^2} (\langle E_{\text{kin}} \rangle - \langle E_{\text{kin}} \rangle_0). \quad (5)$$

Evaluating  $G_3(q)$  Iwamoto, Krotscheck, and Pines found that the functional behavior of  $G_{\text{MC}}(q)$  and  $G_3(q)$  is quite different (see Fig. 1). They concluded that the difference between  $G_{\text{MC}}(q)$ , which was chosen to yield agreement with  $S_{\text{MC}}(q)$ , and  $G_3(q)$ , which was constructed to recover the third-frequency-moment sum rule, is an indication of the importance of dynamic multipair excitations for the electron gas at metallic densities. They reasoned that multipair excitations generally involve significantly greater amounts of energy transfer than either the

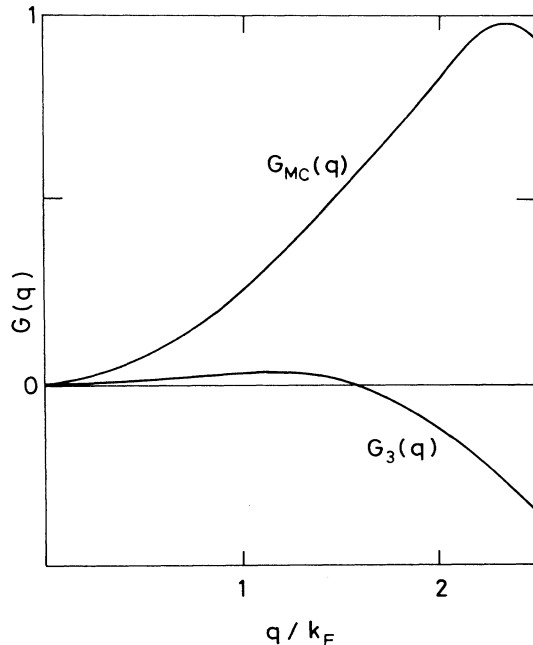


FIG. 1. The local fields  $G_3(q)$  and  $G_{\text{MC}}(q)$  for density  $r_s = 2$  (Ref. 6).

single-pair or collective plasmon excitations. As a consequence, because of the  $\omega^3$  weighting appearing in the integrand of the third-moment sum rule, the effect of multipair excitations on the third-moment sum rule is relatively much greater than their effect on the static structure factor  $S(q)$ .

In this paper we use the microscopic theory of the interacting-electron gas developed by Green, Neilson, and Szymański<sup>8</sup> (GNS) to quantitatively investigate these and related ideas. Since the GNS theory is of the Goldstone perturbation type, it is possible to explicitly identify the separate single-pair, collective mode (plasmon), and multipair terms contributing to the perturbation expansion. We are therefore able, for example, to look at the relative importance of these effects in the self-energy insertions affecting the response function. In the light of our previous discussion, it is also of interest to examine the effect of the different excitation modes on the frequency moment sum rules. A brief report of some of this work has already appeared.<sup>9</sup>

The plan of the paper is as follows. In Sec. II we recall briefly some of the relevant features of the GNS theory. In Sec. III the three excitation modes in the Goldstone diagram language of GNS are defined, and in Sec. IV the separate single-pair and multipair contributions to the dynamic structure factor  $S(q, \omega)$  for large momentum transfers  $q \gg k_F$  are calculated. Section V discusses in detail the frequency moment sum rules, and Sec. VI contains some concluding remarks.

## II. MICROSCOPIC THEORY

The GNS theory was constructed out of an infinite subset of perturbation contributions to the ground-state correlation energy  $\Phi[G]$ , treated as a functional of the self-consistent single-particle propagator  $G$ . Provided  $\Phi[G]$  satisfies certain straightforward symmetry requirements and provided also that the self-energies and the polarization function are generated by functionally differentiating  $\Phi[G]$ , then the theory satisfies the requirements of Baym and Kadanoff<sup>10</sup> for a conserving theory. What this means is that the relationship between the approximate quantities such as density fluctuations and currents in the theory precisely mirrors the relationship between the corresponding exact quantities. For example, the equation of continuity within the theory is exactly satisfied even though the density and current are themselves approximate.

The terms in the GNS theory satisfy these symmetry requirements. They were selected in such a way that the theory is exact for metallic densities in the limits of both small and large momentum transfer. The constraints of exactly satisfying all the conservation relations should then maintain the accuracy of the theory in the momentum-transfer range lying between these two limits.

It has been pointed out by Goodman and Sjölander<sup>11</sup> that the third-frequency-moment sum rule is a consequence of local conservation rather than global conservation, and this means that it is not obvious that a theory satisfying the above criteria must necessarily satisfy this sum rule. Much of Sec. V is devoted to a proof that in fact all theories of the conserving Baym-Kadanoff type do

exactly satisfy the third-frequency-moment sum rule.

We now very briefly outline the steps involved in calculating the dynamic structure factor  $S(q, \omega)$  in the GNS theory.  $S(q, \omega)$  is related to  $\chi^{\text{sc}}(q, \omega)$  through Eq. (2).

To calculate  $\chi^{\text{sc}}$  we first express the exact ground-state energy  $\Phi[G]$  as a function of the fully dressed one-body propagator  $G$ . Our primary approximation enters at the next step where we retain only a subset of the terms contributing to  $\Phi[G]$ . The terms retained are shown in Fig. 2. They include all the particle-particle and hole-hole multiple scattering “ladder” diagrams which have been shown<sup>8</sup> to dominate correlations at large momentum transfers. They also include the particle-hole polarization “ring” diagrams which dominate screening correlations at very small momentum transfers. The key property which ensures conservation is that every single-particle propagator  $G$  in these terms is equivalent to every other  $G$ . The energy functional is then invariant under space-time transformations and this ensures that the conservation laws are exactly satisfied.

The single-particle self-energy  $\Sigma[G]$  in this theory must be obtained by functionally differentiating  $\Phi[G]$  with respect to  $G$ . The corresponding one-body equation of motion is then strictly conserving.

The proper polarization function  $\chi^{\text{sc}}(q, \omega)$  is given by the trace of the proper electron-hole polarization propagator  $\Lambda^{\text{sc}}[G]$  over its single-particle label.  $\Lambda^{\text{sc}}[G]$  is the solution of an integral equation which contains in its kernel a dynamical two-body interaction  $\Xi^{\text{sc}}[G] = i(\delta\Sigma/\delta G) - V$ . This interaction is itself a functional of the self-consistent single-particle propagator  $G$ . In our theory, multi-pair contributions to  $\Lambda^{\text{sc}}[G]$  involving three or more particle excitations can always be broken up into

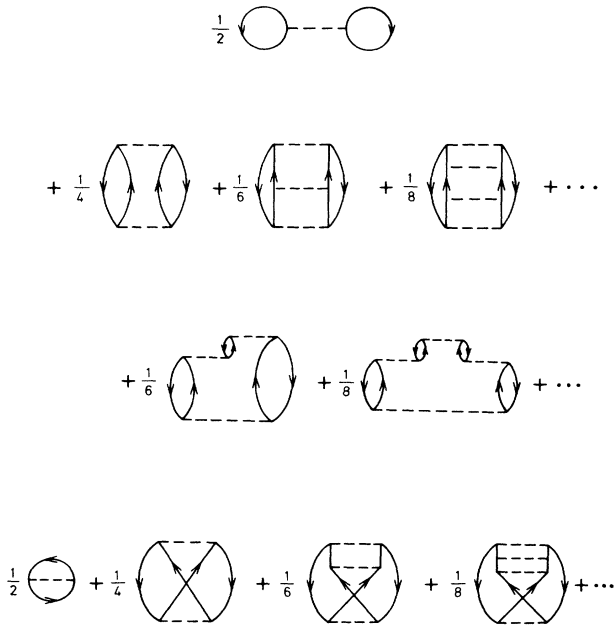


FIG. 2. Contributions to the ground-state functional  $\Phi[G]$  within the present model, with accompanying weighting factors. The horizontal dashed lines are bare Coulomb interactions, the solid lines are self-consistent single-particle propagators.

factors involving single-particle propagators  $G$  and two-body effective interactions  $\Xi^{\text{sc}}[G]$ .

In the next section we specify what we mean by “single pair” and “multipair” in the microscopic language of the GNS theory. We are then in a position to investigate the relative importance of single-pair and multipair effects in the *self-energy*, *particle-hole vertex corrections*, and *t-matrix* contributions to the dynamic structure factor.

### III. SINGLE- AND MULTIPARTICLE EFFECTS

In the microscopic and explicitly time-dependent Goldstone perturbative formalism, multipair effects can easily be identified diagrammatically as terms in which two or more particle-hole excitations exist at the same instant of time. Single-pair corrections to the RPA then operate under the stringent restriction that at no time can more than one particle-hole pair be excited. The explicit time dependence in this diagrammatic representation makes it easy to recognize when a term contains multipair contributions.

The only single-pair corrections to the RPA within the GNS theory are shown in Fig. 3. The two propagators are each fully renormalized with static Hartree-Fock self-energy insertions. The particle-hole vertex corrections involve only unscreened Coulomb interactions. These are summed to infinite order. We can write the proper polarization function arising from all these single-particle effects as

$$\chi_{\text{SP}}(q, \omega) = \frac{\chi^{(0)}(q, \omega)}{1 + V(q)g_{\text{HF}}(q, \omega)\chi^{(0)}(q, \omega)}. \quad (6)$$

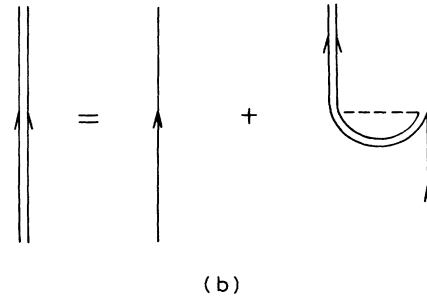
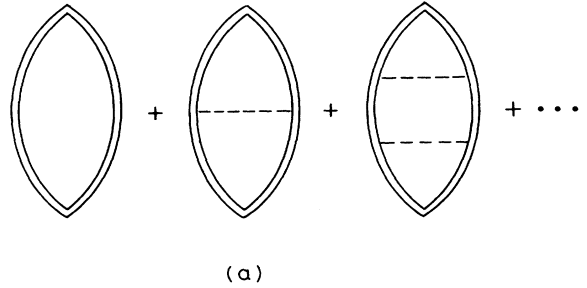


FIG. 3. Complete set of single-pair contributions to the proper polarization function  $\chi^{\text{sc}}(q, \omega)$  within the GNS theory (a). The particle-hole vertex corrections are shown explicitly, while the double lines represent single-particle propagators renormalized with Hartree-Fock self-energies [see (b)].

The Hartree-Fock local field  $g_{\text{HF}}(q, \omega)$  has been calculated to infinite order in the bare Coulomb interaction by Dharma-Wardana and Taylor.<sup>12</sup>

All terms in the GNS set contributing to the proper polarization function which do not appear in Fig. 3 are multipair. These fall into three main categories. First we have *self-energy* effects. We recall the complete GNS set of self-energy insertions  $\Sigma(p, p^0)$ , which includes both single-pair and multipair contributions, consists of the RPA self-energies together with the self-energies associated with *t*-matrix ladders of unscreened Coulomb interactions (see Fig. 4), plus the corresponding exchange terms. The presence of any self-energy insertion beyond the static Hartree-Fock approximation makes the term multipair. The second category consists of the particle-hole *vertex corrections*, which incorporates all those terms involving the scattering of the particle and the hole associated with a single polarization bubble. In this case, it is the screening of the interaction which leads to multipair effects (see Fig. 5). The third category are the *t*-matrix type scattering terms between two adjacent particle-hole polarization bubbles (see Fig. 6).

It can be seen by inspection that the *t*-matrix terms have no single-pair components, but the GNS self-energies and particle-hole vertex correction terms contain a mixture of single-pair and multipair effects. By comparing the single-pair contributions of Fig. 3 with the total contributions, it is possible to obtain a quantitative measure of the multipair contributions.

#### A. Self-energies

Considering first the self-energies, we recall that the fully renormalized single-particle propagator  $G(p, p^0)$  with GNS self-energy insertions  $\Sigma(p, p^0)$  is given by the solution of the Dyson equation

$$G(p, p^0) = G^{(0)}(p, p^0) [1 + \Sigma(p, p^0)G(p, p^0)], \quad (7)$$

where  $G^{(0)}(p, p^0) = (p^0 - p^2/2 \pm i\eta)^{-1}$  is the free-particle propagator. Using the renormalized propagators we can construct the corresponding proper polarization function

$$\chi^{\text{SE}}(q, \omega) = 2 \sum_{\mathbf{k}} \int \frac{dk^0}{2\pi i} G(k, k^0) G(|\mathbf{k} + \mathbf{q}|, k^0 + \omega) \quad (8)$$

$$= 2 \sum_{\mathbf{k}} \int_{E_F}^{\infty} d\omega'' A_{|\mathbf{k} + \mathbf{q}|}(\omega'') \int_{-\infty}^{E_F} d\omega' A_{\mathbf{k}}(\omega') \frac{2(\omega'' - \omega')}{\omega^2 - (\omega'' - \omega' - i\eta)^2}, \quad (9)$$

where  $E_F$  is the Fermi energy, and  $A_{\mathbf{k}}(\omega)$  is the spectral density for the propagator  $G(k, \omega)$ ,

$$A_{\mathbf{k}}(\omega) = \frac{1}{\pi} |G(k, \omega)|^2 |\text{Im}\Sigma(k, \omega)|. \quad (10)$$

Equation (8) includes the total contribution to the proper polarization function from RPA [i.e.,  $\chi^{(0)}(q, \omega)$ ] plus all self-energy insertions, hence the superscript label "SE." As discussed above, the self-energies contain a mixture of

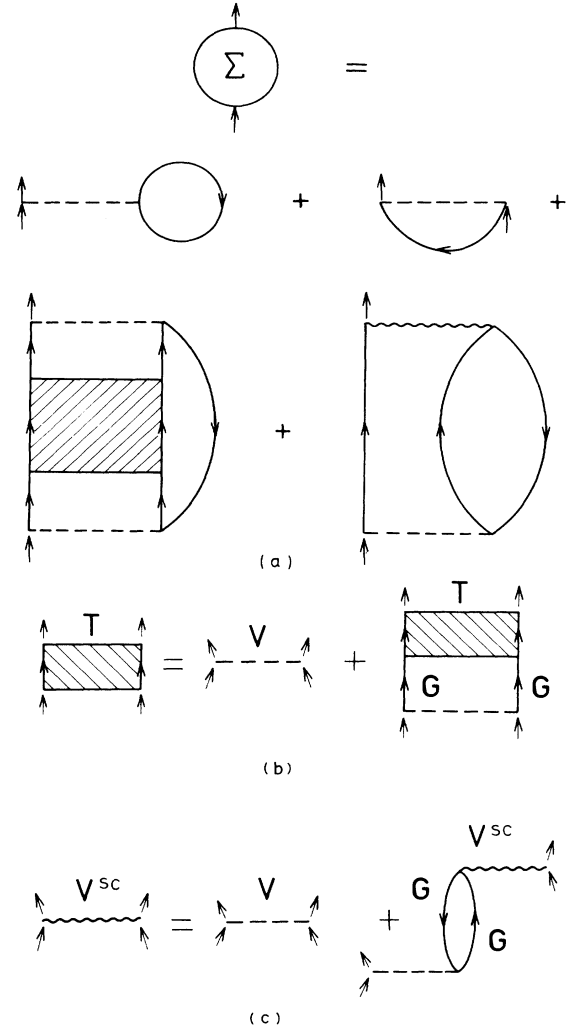


FIG. 4. Self-energy function for the GNS model. This includes both single-pair and multipair contributions. All the propagators are self-consistently renormalized. The hatched box is the dynamic *t*-matrix interaction [see (b)] and the wavy horizontal line is the dynamic RPA screened interaction  $V^{\text{sc}}$  [see (c)].

single-pair and multipair effects.

We can also write down the corresponding spectral density expression when only Hartree-Fock self-energies are included. The corrections to the RPA in this case are purely single-pair. Because the self-energy insertions are static, we can in fact bypass the more elaborate spectral density formalism and immediately express the single-pair contribution to  $\chi^{\text{SE}}(q, \omega)$  from RPA plus self-energy insertions as

$$\chi_{\text{SP}}^{\text{SE}}(q, \omega) = 2 \sum_{\substack{k(<k_F) \\ |\mathbf{k}+\mathbf{q}|>k_F}} \frac{2[\epsilon_{\text{HF}}(|\mathbf{k}+\mathbf{q}|) - \epsilon_{\text{HF}}(k)]}{\omega^2 - [\epsilon_{\text{HF}}(|\mathbf{k}+\mathbf{q}|) - \epsilon_{\text{HF}}(k) - i\eta]^2}, \quad (11)$$

where  $\epsilon_{\text{HF}}(k) = k^2/2 + \Sigma_{\text{HF}}(k)$ . The additional subscript ‘‘SP’’ indicates that only single-pair contributions have been included.

We can now define the net multipair contribution to  $\chi^{\text{SE}}(q, \omega)$  from self-energy insertions as the difference

$$\chi_{\text{MP}}^{\text{SE}}(q, \omega) = \chi^{\text{SE}}(q, \omega) - \chi_{\text{SP}}^{\text{SE}}(q, \omega). \quad (12)$$

### B. Vertex corrections

The vertex correction terms (superscript VC) are associated with particle-hole scattering within a single polarization bubble. If the particle-hole interactions are all unscreened the contribution is single-pair because only one particle-hole excitation is involved. However, if any of the interactions are screened the contribution becomes multipair because of the presence of the additional particle-hole pair excitations in the screened interaction.

In practice one cannot sum the vertex corrections to infinite order if one is using the dynamically screened RPA interaction  $V_{\text{RPA}}(k, k^0)$ . This is because the iterative ladder summation technique cannot be applied for dynamic interactions. When the momentum transfer is large compared with the plasmon cutoff  $q_c$ , an order-by-order comparison of terms reveals that within the single-particle excitation region there is little difference in results between using the dynamic  $V_{\text{RPA}}(k, k^0)$  and using the static bare Coulomb interaction  $V(k)$ . This is due to kinematic constraints which for  $q \gg q_c$  keep all the dynamically screened interactions far from the plasmon pole which exists for  $k \leq q_c$  at  $k^0 \sim \omega_p$ . This means then that within the single-particle excitation region the multipair vertex correction contributions constitute only small corrections to the single-pair contribution.

We may therefore include the effect of multipair particle-hole vertex corrections as a small additional term in the local-field factor  $g(q, \omega)$ ,

$$g(q, \omega) = g_{\text{HF}}(q, \omega) + \delta g_{\text{MP}}^{\text{VC}}(q, \omega). \quad (13)$$

The function  $\delta g_{\text{MP}}^{\text{VC}}(q, \omega)$  is accurately determined by the vertex correction involving a single scattering of the particle and hole via  $V_{\text{RPA}}$  (see Fig. 5). Since  $\delta g_{\text{MP}}^{\text{VC}}(q, \omega)$  is small, we may expand Eq. (1) in powers of it. The contribution to  $\chi^{\text{sc}}$  linear  $\delta g_{\text{MP}}^{\text{VC}}$  is given by

$$\chi_{\text{MP}}^{\text{VC}}(q, \omega) = - \frac{\chi^{(0)}(q, \omega) V(q) \delta g_{\text{MP}}^{\text{VC}}(q, \omega) \chi^{(0)}(q, \omega)}{[1 + V(q) g_{\text{HF}}(q, \omega) \chi^{(0)}(q, \omega)]^2}. \quad (14)$$

This construction continues to work well in the high- $\omega$  region lying beyond the single-particle excitation range: it can be shown that for large momentum transfers the total vertex correction at high  $\omega$  is accurately given by the term of first order in the dynamically screened interaction  $V_{\text{RPA}}$ .<sup>13</sup>

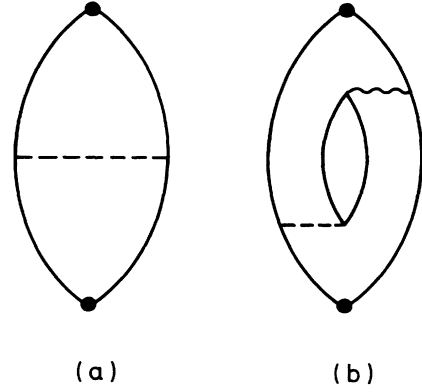


FIG. 5. Particle-hole vertex correction contributions linear in the dynamic two-body interaction  $\Xi^{\text{sc}}$ . (a) represents the single-pair term and (b) represents the multipair term.

### C. $T$ matrix

This category incorporates ladder-type multiple scattering terms between different particle-hole polarization bubbles. In the GNS theory there is a restriction that the multiple scattering occurs between only one pair of adjacent polarization bubbles at any instant of time. These terms necessarily involve the excitation of at least two particle-hole pairs, and so are purely multipair in nature.

Figure 6 shows representative terms for the  $t$ -matrix category in the GNS theory. The corresponding exchange terms are not explicitly shown. Up to second order in the scattering, the interaction is  $V_{\text{RPA}}(q, \omega)$  (wavy lines). For higher orders it is the bare Coulomb interaction  $V(q)$

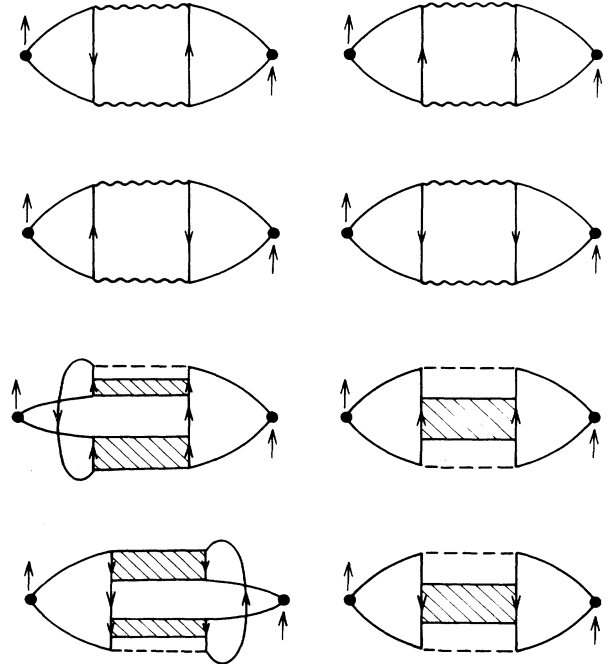


FIG. 6. Representative terms in the  $t$ -matrix category which are linear in the dynamic two-body interaction  $\Xi^{\text{sc}}$ . These terms are purely multipair.

(dotted lines). The diagrams are time ordered and the flow of time is vertically upwards. The dots represent the external vertices. All possible time orderings of the dots relative to the kernel of each diagram must be taken. We write the total contribution from these  $t$ -matrix terms as  $\chi^t(q, \omega)$ .

#### IV. RESULTS

Figure 3 represents all the terms contributing to  $\chi^{\text{sc}}(q, \omega)$  which belong either to the RPA itself or to the single-pair corrections to the RPA. Figure 7 shows for a range of metallic densities the resultant  $S_{\text{SP}}(q, \omega)$ . This is the total single-pair plus collective mode contribution to  $S(q, \omega)$ . Also shown are the corresponding RPA results,  $S_{\text{RPA}}(q, \omega)$ . The central peak of  $S_{\text{SP}}(q, \omega)$  is at a lower value of  $\omega$  than the peak of  $S_{\text{RPA}}(q, \omega)$ . This occurs because the RPA overestimates the potential energy of each particle, the Hartree-Fock exchange correlation corrects for this, and the result is a lower average excitation energy. There are no dissipative effects in  $S_{\text{SP}}(q, \omega)$  and so the curve has a sharp high-energy cutoff which is qualitatively similar to  $S_{\text{RPA}}(q, \omega)$ . However, dispersive effects associated with Hartree-Fock self-energies cause the actual cutoff points to shift. These same dispersive effects also broaden the overall peak of  $S_{\text{SP}}(q, \omega)$  compared to  $S_{\text{RPA}}(q, \omega)$ .

In Fig. 8 we show the multipair contributions from *self-energies*  $\chi_{\text{MP}}^{\text{SE}}(q, \omega)$  from particle-hole *vertex corrections*  $\chi_{\text{MP}}^{\text{VC}}(q, \omega)$ , and from *t-matrix* multiple scattering  $\chi^t(q, \omega)$ . The single-particle excitation region is indicated on the energy scale. For these momentum transfers self-energies and *t*-matrix terms are both significant in the single-particle excitation region, while the particle-hole vertex corrections are small. However, outside the single-particle excitation region, all three categories make important contributions to high-energy tails. The tails arise from dissipative processes which can only occur when multipair excitations are present. The high-energy tails of the self-energies and the particle-hole vertex corrections both fall off as  $(\omega_p^4/8\pi^2)\omega^{-7/2}$ . There is leading order cancellation between the tails of these two terms resulting in a net  $(\omega_p^4/24\pi^2)q^2\omega^{-9/2}$  falloff. A similar pattern can be found in the *t*-matrix terms, which fall off as  $-(\omega_p^4/24\pi^2)q^2\omega^{-9/2}$ . Bringing this tail together with the combined self-energy plus particle-hole vertex correction tail leads to a final net falloff of  $(23\omega_p^4/240\pi^2)q^4\omega^{-11/2}$ . From a practical point of view these cancellations are vital for the satisfaction of the third-moment sum rule. By inspection this sum rule will actually diverge unless the high-energy tail falls off faster than  $\omega^{-4}$ .

In Fig. 9 we compare the total single-pair and multipair contributions to the dynamic structure factor,  $S_{\text{SP}}(q, \omega)$  and  $S_{\text{MP}}(q, \omega)$ , respectively.  $S_{\text{SP}}(q, \omega)$  is the familiar

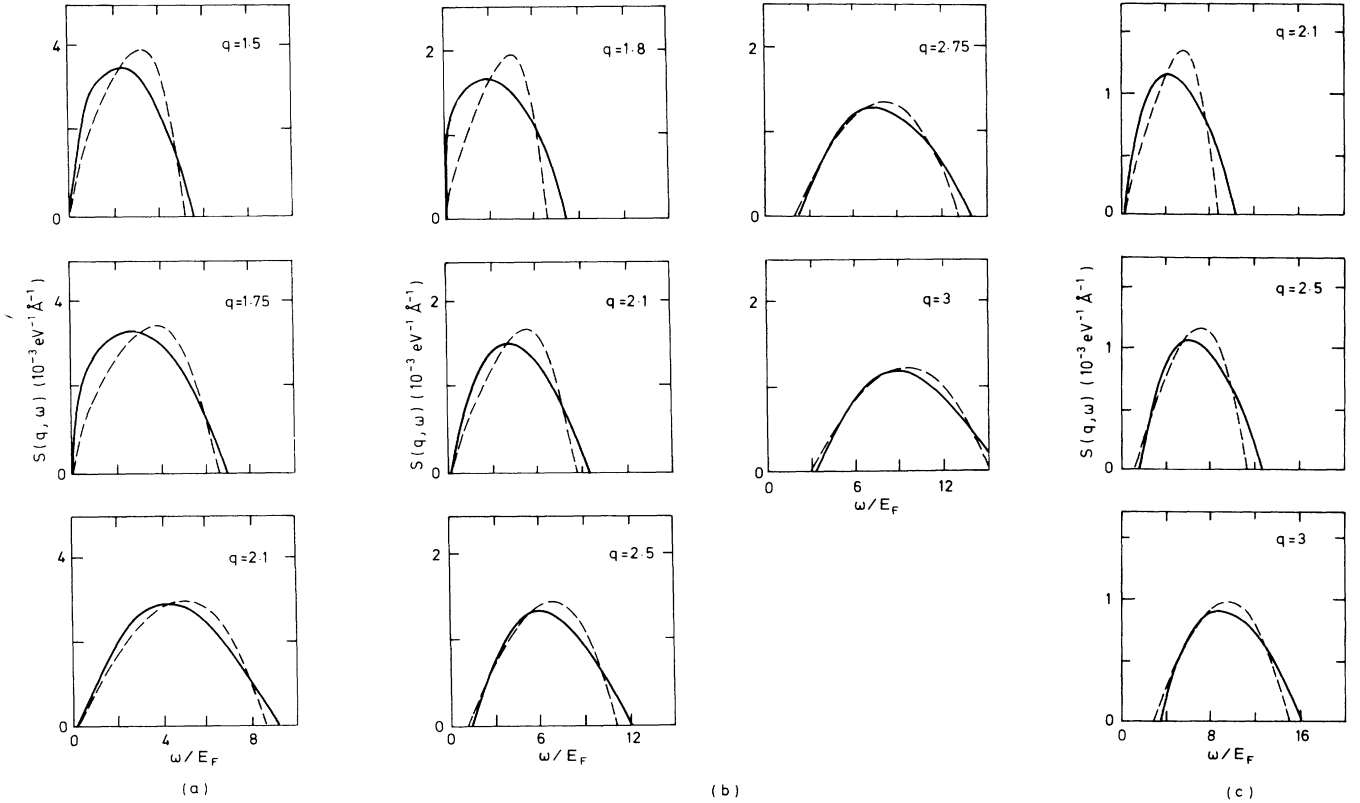


FIG. 7. Dynamic structure factor from all single-pair contributions  $S_{\text{SP}}(q, \omega)$  (solid line). Also shown is  $S_{\text{RPA}}(q, \omega)$  (dashed line). Momentum transfer  $q$  here is in units of  $k_F$ . (a) Density,  $r_s = 1.87$ . (b) Density,  $r_s = 3.22$ . (c) Density,  $r_s = 4$ .

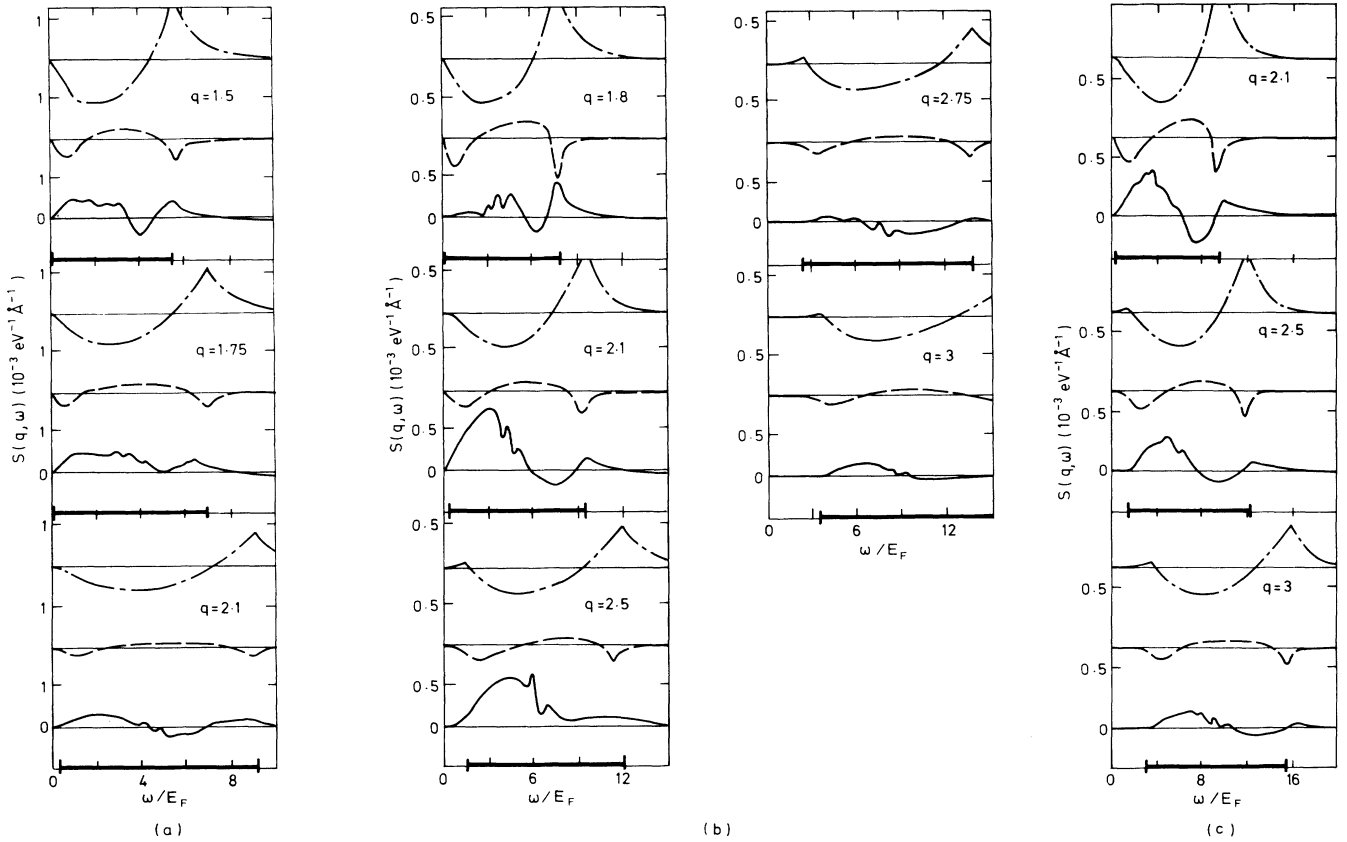


FIG. 8. Multipair contributions to  $\chi^{\text{sc}}(q, \omega)$ . Dot-dashed line is the self-energy contribution  $\chi^{\text{SE}}(q, \omega)$ . Dashed line is the particle-hole vertex correction contribution  $\chi_{\text{MP}}^{\text{VC}}(q, \omega)$ . The solid line is the  $t$ -matrix contribution  $\chi^t(q, \omega)$ . The single-particle excitation range is shown emphasized on the energy scale. (a) Density,  $r_s = 1.87$ . (b) Density,  $r_s = 3.22$ . (c) Density,  $r_s = 4$ .

smooth one-peak curve which has a sharp cutoff at the boundary of the single-particle excitation region. We see that while  $S_{\text{MP}}(q, \omega)$  is smaller than  $S_{\text{SP}}(q, \omega)$  within the single-particle excitation region, it is by no means negligible even for densities as high as  $r_s = 1.87$ . The rich multiple-peak structure in  $S_{\text{MP}}(q, \omega)$  has a dramatic effect on the total  $S(q, \omega)$  in the single-particle excitation region. Outside this region, only  $S_{\text{MP}}(q, \omega)$  is nonzero, so that the high-energy tail of the total  $S(q, \omega)$  also falls off as  $(23\omega_p^4/240\pi^2)q^4\omega^{-11/2}$ .

## V. SUM RULES

In the preceding sections we have dissected the different terms contributing to the dynamic structure factor  $S(q, \omega)$ . We noted the vital role played by multipair effects in ensuring that the third-frequency-moment sum rule converges [Eq. (3)]. Convergence alone, of course, does not ensure that the sum rule is satisfied.

It is easy to show that any conserving formalism of the Baym-Kadanoff type must satisfy the  $f$ -sum rule,

$$\int_0^\infty S(q, \omega) \omega d\omega = nq^2/2. \quad (15)$$

This follows from the well-known link between this sum

rule and particle number conservation. However, it is not immediately clear that such theories must also satisfy the third-frequency-moment sum rule. First of all this sum rule is related only to local conservation in transient times following a collision<sup>11</sup> and not to any overall conservation requirement. Second, there is an initial ambiguity in any approximate theory over which static structure factor  $S(k)$  to use on the right-hand side of Eq. (3). One can either obtain  $S(k)$  by Fourier transforming the instantaneous pair correlation function  $g(r)$ ,

$$S(k) - 1 = n \int d^3r [g(r) - 1] e^{ik \cdot r}, \quad (16)$$

or one can take the zero-time-interval Fourier transform of the dynamic structure factor

$$S(k) = \frac{1}{n} \int_0^\infty d\omega S(k, \omega). \quad (17)$$

For the  $f$ -sum rule this ambiguity does not arise because the right-hand side involves only the simple and exactly-known term  $nq^2/2$ , but in Eq. (3) it is not obvious *a priori* which of the two  $S(k)$  should be used [it is *only* in the exact diagrammatic theory that Eqs. (16) and (17) become equivalent<sup>14</sup>].

In this section we demonstrate for the first time that

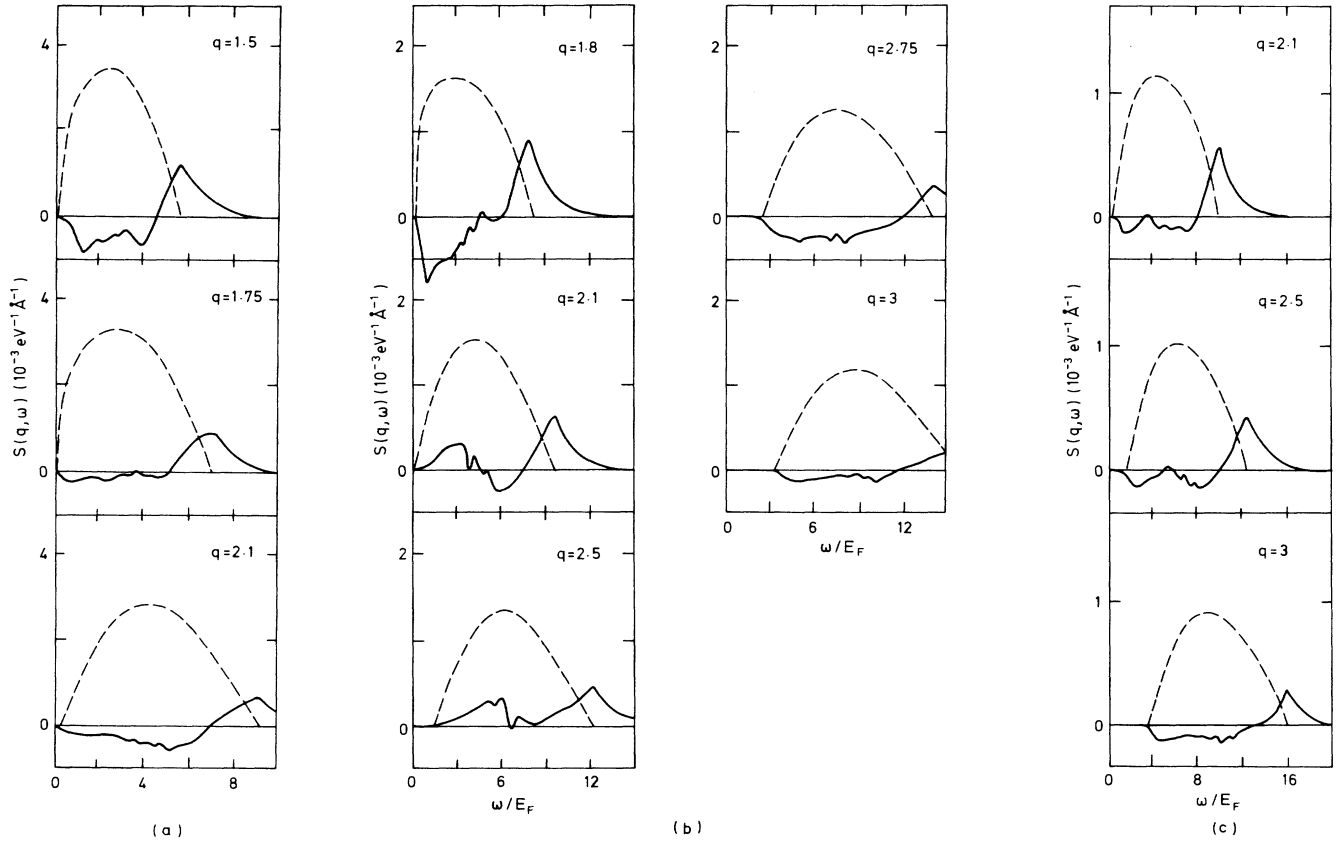


FIG. 9. Total multipair contributions to the dynamic structure factor  $S_{MP}(q, \omega)$  (solid curve), compared with total single-pair contributions  $S_{SP}(q, \omega)$  (dashed curve). (a) Density,  $r_s = 1.87$ . (b) Density,  $r_s = 3.22$ . (c) Density,  $r_s = 4$ .

any conserving theory of the Baym-Kadanoff type does in fact exactly satisfy the third-frequency-moment sum rule. Further, we show that the  $S(k)$  which must be used on the right-hand side of the same rule is determined from Eq. (16), with the  $g(r)$  calculated within the theory.

The proof uses the symmetry properties of the equation of motion for the one-body propagator  $G$ ,

$$\left[ i \frac{\partial}{\partial t_{(\lambda)}} + \frac{1}{2} \nabla_{(\lambda)}^2 \right] G_{(\lambda)\mu} = \Sigma_{\lambda\beta} G_{\beta\mu} + (I_{\alpha\beta} U_{\alpha\beta}) I_{\lambda\beta} G_{\alpha\mu}. \quad (18)$$

We use the implicit summation convention for repeated indices unless they are enclosed in parentheses.  $\Sigma_{\lambda\beta}$  is the self-energy,  $I_{\lambda\beta}$  the unit matrix, and the nonlocal external perturbation we use here is

$$U_{\alpha\beta} = \phi_{\alpha} + \mathbf{A}_{(\alpha)} \cdot \mathbf{P}_{(\alpha)\beta}, \quad (19)$$

where  $\phi$  couples to the density and  $\mathbf{A}$  couples to the current. The momentum operator is defined as

$$\mathbf{P}_{\alpha\beta} = (\nabla_{\alpha} - \nabla_{\beta}) / 2i. \quad (20)$$

Subtracting its adjoint from Eq. (18) and taking the limit  $\mu \rightarrow \lambda^+$ , we find that the  $\Sigma_{\lambda\beta} G_{\beta\mu}$  terms cancel because of the symmetry properties required by the Baym-Kadanoff formalism. The terms involving the local po-

tential  $\phi_{\alpha}$  also cancel, leaving

$$i \frac{\partial}{\partial t_{(\lambda)}} G_{(\lambda\lambda^+)} + i \nabla_{(\lambda)} \cdot \mathbf{P}_{(\lambda\lambda^+)} G_{(\lambda\lambda^+)} = -i \nabla_{(\lambda)} \cdot (\mathbf{A}_{(\lambda)} G_{(\lambda\lambda^+)}) . \quad (21)$$

We identify the density  $\rho$  and the current  $\mathbf{J}$ ,

$$\begin{aligned} \rho_{\lambda} &= -i G_{(\lambda\lambda^+)}, \\ \mathbf{J}_{\lambda} &= -i \mathbf{P}_{(\lambda\lambda^+)} G_{(\lambda\lambda^+)}. \end{aligned} \quad (22)$$

Taking variations of Eq. (21) with respect to  $\phi_{\eta}$  and  $\mathbf{A}_{\eta}$ , we obtain in the limit as  $\phi$  and  $\mathbf{A}$  approach zero,

$$\begin{aligned} \frac{\partial}{\partial t_{(\lambda)}} \chi_{(\lambda)\eta}^{\rho\rho} + \nabla_{(\lambda)} \cdot \vec{\chi}_{(\lambda)\eta}^{J\rho} &= 0, \\ \frac{\partial}{\partial t_{(\lambda)}} \chi_{(\lambda)\eta}^{\rho J} + \nabla_{(\lambda)} \cdot \vec{\chi}_{(\lambda)\eta}^{JJ} &= -\rho_{(\lambda)} \nabla_{(\lambda)} I_{(\lambda)\eta}. \end{aligned} \quad (23)$$

Here  $\chi_{\lambda\eta}^{\rho\rho}$  is the density-density correlation function and  $\vec{\chi}_{\lambda\eta}^{JJ}$  is the current-current correlation function. The other two correlation functions relating density and current obey the relation  $\chi_{\lambda\eta}^{\rho J} = \chi_{\eta\lambda}^{J\rho}$ . This relation follows from the symmetries required by the Baym-Kadanoff framework. Using this property with Eqs. (23) and Fourier transforming, we obtain the relation

$$\chi^{\rho\rho}(\mathbf{q},\omega) = \frac{q^2}{\omega^2}n + \frac{\mathbf{q}\cdot\vec{\chi}^{JJ}(\mathbf{q},\omega)\cdot\mathbf{q}}{\omega^2}. \quad (24)$$

We demonstrate in the Appendix that

$$\lim_{\omega\rightarrow\infty} \mathbf{q}\cdot\vec{\chi}^{JJ}(\mathbf{q},\omega)\cdot\mathbf{q} = \frac{q^2}{\omega^2}M_3(q) + \dots, \quad (25)$$

so that in the large- $\omega$  limit, Eq. (24) becomes

$$\lim_{\omega\rightarrow\infty} \chi^{\rho\rho}(\mathbf{q},\omega) = \frac{q^2}{\omega^2}n + \frac{q^2}{\omega^4}M_3(q) + \dots. \quad (26)$$

The Kramers-Krönig dispersion relations imply that

$$\begin{aligned} \lim_{\omega\rightarrow\infty} \text{Re}\chi^{\rho\rho}(\mathbf{q},\omega) &= \lim_{\omega\rightarrow\infty} \left[ -2 \mathcal{P} \int_0^\infty \frac{d\omega'}{\pi} \frac{\omega' \text{Im}\chi^{\rho\rho}(\mathbf{q},\omega')}{\omega^2 - \omega'^2} \right] \\ &= -\frac{2}{\omega^2} \int_0^\infty \int_0^\infty \frac{d\omega'}{\pi} \omega' \text{Im}\chi^{\rho\rho}(\mathbf{q},\omega') - \frac{2}{\omega^4} \int_0^\infty \frac{d\omega'}{\pi} (\omega')^3 \text{Im}\chi^{\rho\rho}(\mathbf{q},\omega') + O(\omega^{-6}). \end{aligned} \quad (27)$$

By combining Eqs. (26) and (27) we recover the  $f$ -sum rule

$$\int_0^\infty \frac{d\omega'}{\pi} \omega' [-\text{Im}\chi^{\rho\rho}(\mathbf{q},\omega')] = \frac{nq^2}{2}, \quad (28)$$

and the third-frequency-moment sum rule

$$\int_0^\infty \frac{d\omega'}{\pi} (\omega')^3 [-\text{Im}\chi^{\rho\rho}(\mathbf{q},\omega')] = \frac{q^2 M_3(q)}{2}. \quad (29)$$

In the Appendix we evaluate the function  $M_3(q)$ , and confirm that

$$M_3(q) = \frac{nq^4}{4} + 2nq^2 \langle E_{\text{kin}} \rangle + 4\pi e^2 n^2 \left[ 1 - \frac{1}{n} \int \frac{d^3k}{(2\pi)^3} (\hat{\mathbf{q}}\cdot\hat{\mathbf{k}})^2 [S(k) - S(|\mathbf{q}-\mathbf{k}|)] \right], \quad (30)$$

where the  $S(k)$  here must be taken from the Fourier transform of the calculated model pair correlation function [see Eq. (16)].

We conclude that both the  $f$ -sum rule and the third-frequency-moment sum rule are exactly satisfied by an approximate theory which satisfies the Baym-Kadanoff conserving requirement. In the GNS theory this means that the delicate cancellations we have already noted among the different multipair terms in the high- $\omega$  tail do not merely enforce convergence on the third-frequency-moment integral, but actually ensure that the sum rule itself is exactly maintained when all the dynamic multipair corrections to the RPA are incorporated.

## VI. SUMMARY AND CONCLUSIONS

The main points to emerge from this paper are as follows.

(i) That multipair effects significantly affect the dynamic response function even at the highest metallic densities.

(ii) Two very important effects which are purely multipair are the multiple peaks in the dynamic structure factor and the asymptotic falloff of the tail of  $S(q,\omega)$  in the

high- $\omega$  region outside the single-particle excitation range.

(iii) The form of the asymptotic falloff of the high- $\omega$  tails is determined by delicate cancellations among quite different terms: self-energy, particle-hole vertex correction, and  $t$ -matrix. The third-frequency-moment sum rule is particularly sensitive to the tails. Unless a theory correctly takes into account these cancellations, it is most unlikely that it will satisfy the sum rule.

## ACKNOWLEDGMENTS

We are grateful to M. W. C. Dharma-Wardana and R. Taylor for providing us with full details of their Hartree-Fock calculation, and we thank them and also N. Iwamoto and R. A. Smith for helpful discussions. One of us (F.G.) thanks the Aspen Center for Physics for its hospitality. Finally, D.P. acknowledges support from the University of New South Wales Gordon Godfrey Bequest.

## APPENDIX

In this appendix we determine the form of the function  $M_3(q)$  appearing in Eq. (29). Multiplying Eq. (18) by the momentum operator  $\mathbf{P}_{\lambda\mu}$ , and taking the limit  $\mu \rightarrow \lambda^+$  we obtain

$$\begin{aligned} i \left[ \frac{\partial}{\partial t_{(\lambda)}} + \nabla_{(\lambda)} \cdot \mathbf{P}_{(\lambda\lambda^+)} \right] \mathbf{P}_{(\lambda\lambda^+)} G_{(\lambda\lambda^+)} &= -i (\nabla_{(\lambda)} \phi_{(\lambda)}) G_{(\lambda\lambda^+)} - i (\nabla_{(\lambda)} \mathbf{A}_{(\lambda)}) \cdot \mathbf{P}_{(\lambda\lambda^+)} G_{(\lambda\lambda^+)} \\ &\quad - i \nabla_{(\lambda)} (\cdot \mathbf{A}_{(\lambda)}) \cdot \mathbf{P}_{(\lambda\lambda^+)} G_{(\lambda\lambda^+)} + \mathbf{P}_{(\lambda\lambda^+)} (\Sigma_{(\lambda)\beta} G_{\beta(\lambda^+)} - G_{(\lambda)\beta} \Sigma_{\beta(\lambda^+)}) . \end{aligned} \quad (A1)$$

Varying Eq. (A1) with respect to  $\mathbf{A}_\eta$ , and letting  $\mathbf{A}$  and  $\phi$  approach zero, we are left with

$$i \left[ \frac{\partial}{\partial t_{(\lambda)}} + \nabla_{(\lambda)} \cdot \mathbf{P}_{(\lambda\lambda+)} \right] \vec{\chi}_{(\lambda)\eta}^{JJ} = -i \frac{\delta}{\delta \mathbf{A}_\eta} \mathbf{P}_{(\lambda\lambda+)} (\Sigma_{(\lambda)\beta} G_{\beta(\lambda+)} - G_{(\lambda)\beta} \Sigma_{\beta(\lambda+)}) . \quad (\text{A2})$$

Let us now examine the right-hand side of Eq. (A2). We first split the self-energy  $\Sigma_{\alpha\beta}$  into its Hartree component  $\Sigma_{\alpha\beta}^H$  and its correlation component  $\Sigma_{\alpha\beta}^{\text{sc}}$

$$\begin{aligned} \Sigma_{\alpha\beta} &= \Sigma_{\alpha\beta}^H + \Sigma_{\alpha\beta}^{\text{sc}} , \\ \Sigma_{\alpha\beta}^H &= I_{\beta\alpha} V_{\alpha\gamma} (-iG_{\gamma\gamma+}) , \\ \Sigma_{\alpha\beta}^{\text{sc}} &= -iG_{\beta\alpha'} V_{\alpha'(\alpha)} (iG_{\alpha\rho'} G_{(\alpha)\rho}) \xi_{\rho\rho',\beta\beta'}^{\text{sc}} , \end{aligned} \quad (\text{A3})$$

where  $\xi_{\rho\rho',\beta\beta'}^{\text{sc}}$  is the two-body effective interaction appearing in  $\Phi[G]$ . The contribution of  $\Sigma_{\alpha\beta}^H$  on the right-hand side of Eq. (A2) can be written

$$\begin{aligned} \frac{\delta}{\delta \mathbf{A}_\eta} \mathbf{P}_{(\lambda\lambda+)} (\Sigma_{(\lambda)\beta}^H G_{\beta(\lambda+)} - G_{(\lambda)\beta} \Sigma_{\beta(\lambda+)}^H) &= i \nabla_{(\lambda)} V_{(\lambda)\gamma} \left[ i \frac{\delta G_{\gamma\gamma+}}{\delta \mathbf{A}_\eta} G_{(\lambda\lambda+)} + iG_{\gamma\gamma+} \frac{\delta G_{(\lambda\lambda+)}}{\delta \mathbf{A}_\eta} \right] \\ &= n \nabla_{(\lambda)} V_{(\lambda)\gamma} \chi_{\gamma\eta}^{\rho J} , \end{aligned} \quad (\text{A4})$$

where we have used the property that  $\nabla_{(\lambda)} V_{(\lambda)\gamma}$  is an odd function of  $\gamma$ .

Returning to the complete expression for the right-hand side of Eq. (A2), the remaining term which has to be evaluated is

$$\begin{aligned} \frac{\delta}{\delta \mathbf{A}_\eta} \mathbf{P}_{(\lambda\lambda+)} (\Sigma_{(\lambda)\beta}^{\text{sc}} G_{\beta(\lambda+)} - G_{(\lambda)\beta} \Sigma_{\beta(\lambda+)}^{\text{sc}}) &= - \frac{\delta}{\delta \mathbf{A}_\eta} \mathbf{P}_{(\lambda\lambda+)} (V_{(\lambda)\lambda'} - V_{(\lambda+)\lambda'}) (-iG_{\beta(\lambda+)} G_{(\lambda)\xi} \xi_{\xi\xi',\beta\beta'}^{\text{sc}} (-iG_{\beta\lambda'+} G_{\lambda'\xi'}) \\ &= i (\nabla_{(\lambda)} V_{(\lambda)\lambda'}) \frac{\delta}{\delta \mathbf{A}_\eta} [(-iG_{\beta(\lambda+)} G_{(\lambda)\xi} \xi_{\xi\xi',\beta\beta'}^{\text{sc}} (-iG_{\beta\lambda'+} G_{\lambda'\xi'})] . \end{aligned} \quad (\text{A5})$$

Noting that eventually we shall Fourier transform Eq. (A2) and take its high-frequency limit, we can simplify the discussion at this point by introducing an approximation which becomes exact when the high-frequency limit is taken:

$$\frac{\delta}{\delta \mathbf{A}_\eta} = \frac{\delta G_{\mu\nu}}{\delta \mathbf{A}_\eta} \frac{\delta}{\delta G_{\mu\nu}} \approx \mathbf{P}_{(\eta\eta+)} G_{\mu(\eta+)} G_{(\eta)\nu} \frac{\delta}{\delta G_{\mu\nu}} . \quad (\text{A6})$$

The expression in Eq. (A5) can then be written

$$\begin{aligned} i (\nabla_{(\lambda)} V_{(\lambda)\lambda'}) \mathbf{P}_{(\eta\eta+)} \{ [(-iG_{\beta(\eta+)} G_{(\eta\lambda+)}) G_{(\lambda)\xi} + (-iG_{(\lambda\eta+)} G_{(\eta)\xi}) G_{\beta(\lambda+)}] \xi_{\xi\xi',\beta\beta'}^{\text{sc}} (-iG_{\beta\lambda'+} G_{\lambda'\xi'}) \\ + (-iG_{\beta(\lambda+)} G_{(\lambda)\xi} \xi_{\xi\xi',\beta\beta'}^{\text{sc}} [(-iG_{\beta(\eta+)} G_{(\eta)\lambda'+}) G_{\lambda'\xi'} + (-iG_{\lambda'(\eta+)} G_{(\eta)\xi'}) G_{\beta\lambda'+}] \} . \end{aligned} \quad (\text{A7})$$

We have again anticipated taking the limit  $\omega \rightarrow \infty$  by neglecting the derivative  $\delta \xi^{\text{sc}} / \delta G$ , which becomes negligible in this limit.

By defining

$$F_{\xi\beta,\lambda'} = \xi_{\xi\xi',\beta\beta'}^{\text{sc}} (-iG_{\beta(\lambda'+)} G_{(\lambda')\xi'}) \quad (\text{A8})$$

and using the properties

$$\begin{aligned} \vec{\chi}_{\lambda\eta}^{JJ} &= \mathbf{P}_{(\lambda\lambda+)} \mathbf{P}_{(\eta\eta+)} \chi_{(\lambda)\eta}^{\rho\rho} , \\ \nabla_{(\eta)} \cdot \chi_{\gamma(\eta)}^{\rho J} &= - \frac{\partial}{\partial t_{(\eta)}} \chi_{\gamma(\eta)}^{\rho\rho} , \end{aligned} \quad (\text{A9})$$

we may now use Eq. (A2) and the results expressed in Eqs. (A4) and (A7) to obtain an expression for the longitudinal part of the current-current correlation function:

$$\begin{aligned} \chi_{\lambda\eta}^L &= \nabla_{(\lambda)} \nabla_{(\eta)} \cdot \vec{\chi}_{(\lambda)\eta}^{JJ} , \\ i \frac{\partial}{\partial t_{(\lambda)}} \chi_{(\lambda)\eta}^L &= -i \nabla_{(\lambda)} \cdot \mathbf{P}_{(\lambda\lambda+)} \nabla_{(\lambda)} \cdot \mathbf{P}_{(\lambda\lambda+)} \nabla_{(\eta)} \cdot \mathbf{P}_{(\eta\eta+)} \chi_{(\lambda)\eta}^{\rho\rho} + in \nabla_{(\lambda)}^2 V_{(\lambda)\gamma} \frac{\partial}{\partial t_{(\eta)}} \chi_{\gamma(\eta)}^{\rho\rho} \\ &\quad - i \nabla_{(\lambda)} \cdot \{ (\nabla_{(\lambda)} V_{(\lambda)\lambda'}) \nabla_{(\eta)} \cdot \mathbf{P}_{(\eta\eta+)} [ (G_{\beta(\eta+)} G_{(\eta\lambda+)} G_{(\lambda)\xi} + G_{(\lambda\eta+)} G_{(\eta)\xi} G_{\beta(\lambda+)} ) F_{\xi\beta,\lambda'} \\ &\quad + F_{\xi\beta',(\lambda)} (G_{\beta(\eta+)} G_{(\eta)\lambda'+} G_{\lambda'\xi'} + G_{\lambda'(\eta+)} G_{(\eta)\xi'} G_{\beta\lambda'+}) ] \} . \end{aligned} \quad (\text{A11})$$

We note that, for a uniform system,  $F_{\xi\beta,\lambda'}$  is a function of  $(\xi - \lambda')$  and  $(\lambda' - \beta)$  only. Adopting the abbreviated notation  $p \equiv (\mathbf{p}, p^0)$  and taking the Fourier transform of Eq. (A11), we obtain

$$\begin{aligned}
\omega \mathbf{q} \cdot \vec{\chi}^{JJ}(\mathbf{q}, \omega) \cdot \mathbf{q} = \omega \chi^L(\mathbf{q}, \omega) = & -2i \int \frac{d^4 p}{(2\pi)^4} G(p) G(p+q) \left[ \frac{p^2 - (\mathbf{p} + \mathbf{q})^2}{2} \right]^2 \left[ \frac{(\mathbf{p} + \mathbf{q})^2 - p^2}{2} \right] + nq^2 V(\mathbf{q}) \omega \chi^{\rho\rho}(\mathbf{q}, \omega) \\
& - 2 \int \frac{d^4 p}{(2\pi)^4} \int \frac{d^4 k}{(2\pi)^4} \mathbf{q} \cdot \mathbf{k} V(\mathbf{k}) \{ [G(p)G(p+k)G(p+k+q) \mathbf{q} \cdot (\mathbf{p} + \mathbf{k} + \mathbf{q}/2) \\
& + G(p)G(p+k)G(p-q) \mathbf{q} \cdot (\mathbf{p} - \mathbf{q}/2)] F(p, k) \\
& - [G(p)G(p+k)G(p+k-q) \mathbf{q} \cdot (\mathbf{p} + \mathbf{k} - \mathbf{q}/2) \\
& + G(p)G(p-q)G(p+k-q) \mathbf{q} \cdot (\mathbf{p} - \mathbf{q}/2)] F(p, k - q) \} .
\end{aligned} \tag{A12}$$

In the limit of high frequencies, Eq. (A12) becomes

$$\begin{aligned}
\lim_{\omega \rightarrow \infty} \omega \mathbf{q} \cdot \vec{\chi}^{JJ}(\mathbf{q}, \omega) \cdot \mathbf{q} = & 2 \int \frac{d^4 p}{(2\pi)^4} (\mathbf{q} \cdot \mathbf{p} + q^2/2)^3 \frac{G(p) - G(p+q)}{\omega} + nq^2 V(\mathbf{q}) \omega \frac{nq^2}{\omega^2} \\
& + 2 \int \frac{d^4 p}{(2\pi)^4} \int \frac{d^4 k}{(2\pi)^4} \mathbf{q} \cdot \mathbf{k} V(\mathbf{k}) \left[ \frac{G(p)G(p+k)}{\omega} F(p, k) \mathbf{q} \cdot (\mathbf{k} + \mathbf{q}) \right. \\
& \left. - \frac{G(p)G(p+k-q)}{\omega} F(p, k - q) \mathbf{q} \cdot \mathbf{k} \right] ,
\end{aligned} \tag{A13}$$

where we have used the properties

$$\lim_{\omega \rightarrow \infty} \omega G(p)G(p+q) = G(p) - G(p+q) \tag{A14}$$

and

$$\begin{aligned}
\lim_{\omega \rightarrow \infty} \omega G(p)G(p+k)G(p+k+q) \\
= G(p)[G(p+k) - G(p+k+q)] ,
\end{aligned} \tag{A15}$$

with  $\omega \equiv q^0$ .

We note that

$$-\frac{1}{n} \int \frac{dk^0}{2\pi i} 2 \int \frac{d^3 p}{(2\pi)^3} G(p)G(p+k)F(p, k) = S(k) \tag{A16}$$

can be identified with the static structure factor which determines the correlation energy  $E_{\text{corr}}$  in the Feynman-

Hellmann integral expression over the coupling strength  $Z$ :

$$E_{\text{corr}} = \frac{1}{2} \int_0^1 \frac{dZ}{Z} \int \frac{d^3 k}{(2\pi)^3} [ZV(k)][S_Z(k) - 1] . \tag{A17}$$

$S_Z(k)$  must be taken from the Fourier transform of the pair correlation function  $g(r)$  calculated directly from  $\Phi[G]$ , and, as we have already noted, is not equal to the zero-time Fourier transform of the dynamic structure factor within the same conserving approximation.<sup>14</sup>

Using Eq. (A16) and recalling that

$$n_p = \int \frac{dp^0}{2\pi i} G(p) e^{ip^0} \tag{A18}$$

is the occupation number for the interacting system, Eq. (A13) simplifies to

$$\begin{aligned}
\lim_{\omega \rightarrow \infty} \omega \mathbf{q} \cdot \vec{\chi}^{JJ}(\mathbf{q}, \omega) \cdot \mathbf{q} = & \frac{2}{\omega} \int \frac{d^3 p}{(2\pi)^3} \left[ \frac{q^6}{4} + 3q^2(\mathbf{q} \cdot \mathbf{p})^2 \right] n_p + 4\pi e^2 n^2 \frac{q^2}{\omega} \\
& - n \int \frac{d^3 k}{(2\pi)^3} \mathbf{q} \cdot \mathbf{k} \frac{4\pi e^2}{k^2} \left[ \frac{S(k)}{\omega} \mathbf{q} \cdot \mathbf{k} - \frac{S(|\mathbf{q} - \mathbf{k}|)}{\omega} \mathbf{q} \cdot \mathbf{k} \right] .
\end{aligned} \tag{A19}$$

All terms on the right side of Eq. (A19) fall off as  $\omega^{-1}$ . Thus we can finally identify the function  $M_3(q)$  which appears in Eqs. (25) and (26):

$$M_3(q) = \frac{nq^4}{4} + q^2 n \langle p^2 \rangle + 4\pi e^2 n^2 \left[ 1 - \frac{1}{n} \int \frac{d^3 k}{(2\pi)^3} (\hat{\mathbf{q}} \cdot \hat{\mathbf{k}})^2 [S(k) - S(|\mathbf{q} - \mathbf{k}|)] \right] , \tag{A20}$$

where the expectation value  $\langle p^2 \rangle$  is obtained by averaging over the interacting Fermi sea.

\*Permanent address.

- <sup>1</sup>A. Miller, P. Nozières, and D. Pines, *Phys. Rev.* **127**, 1452 (1962).
- <sup>2</sup>R. P. Feynman, *Phys. Rev.* **94**, 262 (1954).
- <sup>3</sup>E. Manousakis, D. Pines, and Q. Usmani (unpublished).
- <sup>4</sup>J. Hubbard, *Proc. R. Soc. London, Ser. A* **243**, 336 (1957); K. S. Singwi, A. Sjölander, M. P. Tosi, and R. H. Land, *Phys. Rev. B* **1**, 1044 (1970).
- <sup>5</sup>G. Niklasson, *Phys. Rev. B* **10**, 3052 (1974); A. A. Kugler, *J. Stat. Phys.* **12**, 35 (1975).
- <sup>6</sup>N. Iwamoto, E. Krotscheck, and D. Pines, *Phys. Rev. B* **29**, 3936 (1984).
- <sup>7</sup>D. M. Ceperley and B. J. Alder, *Phys. Rev. Lett.* **45**, 566 (1980).
- <sup>8</sup>F. Green, D. Neilson, and J. Szymański, *Phys. Rev. B* **31**, 2779 (1985); *Phys. Rev. B* **31**, 2796 (1985); *Phys. Rev. B* **31**, 5837 (1985).
- <sup>9</sup>F. Green, D. Neilson, D. Pines, and J. Szymański, in *Recent Progress in Many-Body Theories*, edited by P. J. Siemens and R. A. Smith (Springer, Berlin, 1986).
- <sup>10</sup>G. Baym and L. P. Kadanoff, *Phys. Rev.* **124**, 287 (1961).
- <sup>11</sup>B. Goodman and A. Sjölander, *Phys. Rev. B* **8**, 200 (1973).
- <sup>12</sup>M. W. C. Dharma-Wardana and R. Taylor, *J. Phys. F* **10**, 2217 (1980).
- <sup>13</sup>A. J. Glick and W. F. Long, *Phys. Rev. B* **4**, 3455 (1971).
- <sup>14</sup>A. D. Jackson and R. A. Smith (private communication).